Synthesis and near-infrared luminescence of 3d-4f bi-metallic Schiff base complexes

Wai-Kwok Wong,*[a] Hongze Liang,[a] Wai-Yeung Wong,[a] Zongwei Cai,[a] King-Fai Li[b] and Kok-Wai Cheah[b]

[a] *Department of Chemistry, Hong Kong Baptist University, Waterloo Road, Kowloon Tong, Hong Kong, P.R. China. E-mail: wkwong@hkbu.edu.hk; Phone: +852 2339 7075; Fax: +852 2339 7348*

[b] *Department of Physics, Hong Kong Baptist University, Waterloo Road, Kowloon Tong, Hong Kong, P.R. China*

Received (in Montpellier, France) 11th May 2001, Accepted 20th December 2001
First published as an Advance Article on the web 14th February 2002

The reaction of the zinc(II) Schiff base complex ZnL [H_2L = *N*,*N*′-bis(3-methoxysalicylidene)ethylene-1,2-diamine] with one equivalent of $Ln(NO_3)_3{\cdot}xH_2O$ (Ln = Nd, Ho, Er or Yb) gives the neutral 3d-4f bi-metallic Schiff base complexes $[Zn(NO_3)(\mu\text{-}L)Ln(NO_3)_2(H_2O)]$, which in solution exhibit emission corresponding to the Ln(III) ions (Ln = Nd, Er and Yb) in the near-infrared region.

The potential applications of trivalent lanthanide complexes as contrast agents for magnetic resonance imaging[1] and stains for fluorescence imaging[2] have prompted considerable interest in the preparation, magnetic and optical properties of 3d-4f heterometallic complexes.[3–7] Recently, there has been growing interest in the preparation and magnetic properties of 3d-4f heterometallic Schiff base complexes;[8,9] however, there are relatively few studies on their luminescent properties. This may be due to the fact that some lanthanide ions such as Eu(III) and Tb(III) possess strongly emissive and long-lived excited states but do not exhibit intense absorption bands.[10] Therefore, considerable effort has been devoted to the design of lanthanide complexes in which light is absorbed by the ligands and the corresponding electronic energy is then transferred to the emitting metal ions.[11–15] Currently, there is a great interest in the luminescent properties of erbium(III), ytterbium(III) and neodymium(III) polydentate complexes.[11,13,16–19] These lanthanide(III) ions, which emit in the near-infrared (NIR) region, a region where biological tissues and fluids are relatively transparent, have potential for chemosensor and fluoroimmuno assay applications. The use of transition metal complexes as sensitizers for Nd(III) and Yb(III) luminescence was only reported recently.[20] Zinc(II) Schiff base complexes have been shown to be effective emitters,[21] thus we are interested in exploring them as sensitizers for lanthanide metal ions.

The reaction of the zinc(II) Schiff base complex ZnL [H_2L = *N*,*N*′-bis(3-methoxysalicylidene)ethylene-1,2-diamine] with 1 equiv of $Ln(NO_3)_3{\cdot}xH_2O$ (Ln = Ho, Nd, Er or Yb) gives the neutral 3d-4f bi-metallic Schiff base complexes $[Zn(NO_3)(\mu\text{-}L)Ln(NO_3)_2(H_2O)]$ (Ln = Nd, **1**; Ho, **2**; Er, **3**; and Yb, **4**) in good yields (Scheme 1). The structure of **2** was ascertained by X-ray crystallography and its perspective drawing is shown in Fig. 1. Crystal structure analysis revealed that the relatively soft transition metal ion, Zn(II), is located in the inner N_2O_2 cavity of the Schiff base ligand. The zinc(II) ion is five-fold co-ordinated and adopts a distorted square pyramidal geometry, with the imino nitrogen atoms N(1) and N(2), and the phenolic oxygen atoms O(2) and O(3) forming the square base, while the nitrato oxygen O(5) occupies the axial position. The average length of the Zn–O (phenolic) [2.026(5) Å] and Zn–N [2.032(6) Å] bonds is in the normal range and comparable to those of other similar Zn(II) Schiff base complexes.[22] The Ho(III) and Zn(II) ions are connected by two bridging phenolic oxygen donors, with a separation of 3.446 Å. The Ho(III) ion is nine-fold co-ordinated, surrounded by nine O atoms, two from the bridging phenolic groups, two from the methoxy groups, four from the two bidentate nitrato ligands and one from the aqua ligand. The structure of **2** is very similar to those of the analogous Cu-Gd 3d-4f Schiff base complexes.[8] The major structural difference between **2** and the Cu-Gd complexes is that in **2**, only two of the three nitrato ligands are bidentately coordinated to the lanthanide(III) ion with the third nitrato ligand monodentately coordinated to the Zn(II) ion, while in the Cu-Gd complexes, all three nitrato ligands are bidentately bound to the lanthanide(III) ion.

Compounds **1**–**4** show similar fragmentation pattern in their positive FAB mass spectra, which exhibit the $[M - H_2O - NO_3]^+$ fragment at *m*/*z* 660 (**1**), 679 (**2**), 680 (**3**) and 688 (**4**). This indicates that the monodentate nitrato ligand is easier to detach from the complexes than the bidentate nitrato ligands under the MS experimental conditions. When dissolved in methanol, the electrospray ionization mass spectra (ESI-MS) of compounds **1**–**4** also show similar fragmentation patterns. They exhibit the $[M - H_2O - NO_3]^+$ peak, the $[LnL]^+$ peak (the most abundant peak) at *m*/*z* 472 (**1**), 492 (**2**), 494 (**3**) and 500 (**4**) and a very small $[ZnL + H]^+$ peak at *m*/*z* 391.

Conductivity measurements further revealed that compounds **1**–**4** behaved as strong electrolytes in methanol. For strong electrolytes, $\Lambda_e = \Lambda_0 - B\sqrt{C_{eq}}$,[23] in which Λ_e is the equivalent conductivity, Λ_0 is the equivalent conductivity at infinite dilution, and C_{eq} is the equivalent concentration. For compound **2**, a plot of $(\Lambda_0 - \Lambda_e)$ *vs.* $\sqrt{C_{eq}}$ gave an experimental slope of 789 ± 141 $S{\cdot}L^{1/2}{\cdot}equiv^{-1/2}$.† This value compares favourably to the theoretical slope of 698 $S{\cdot}L^{1/2}{\cdot}equiv^{-1/2}$ determined from the Kohlraush and Onsager equations[23b] for a 2 : 1 electrolyte. The above data suggest that compounds **1**–**4** probably exist as $[Zn(\mu\text{-}L)Ln(NO_3)(solvent)_x][NO_3]_2$ in solution.

At room temperature, compounds **1**–**4** also exhibit similar solution absorption and emission spectra in the UV-VIS region. Their photophysical properties are summarized in Table 1. The absorptions between 272 and 367 nm can be assigned to $\pi \rightarrow \pi^*$ transitions of the Schiff base ligand. The

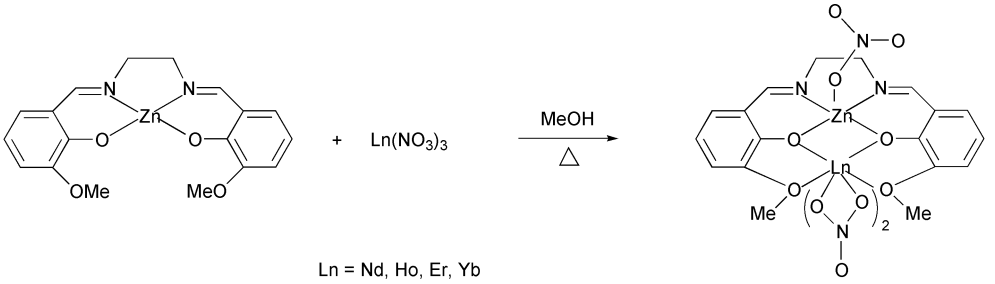

Scheme 1

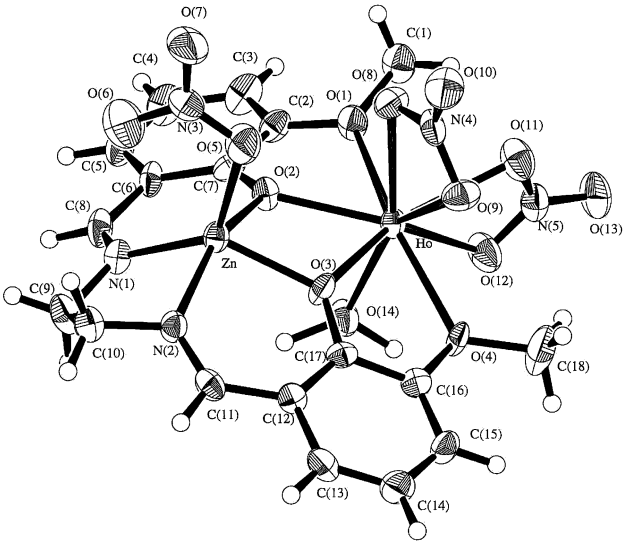

Fig. 1 A perspective drawing of compound **2**. Selected bond lengths (Å) and angles (°): Ho–O(1) 2.531(5), Ho–O(2) 2.266(5), Ho–O(3) 2.293(5), Ho–O(4) 2.487(5), Ho–O(8) 2.436(5), Ho–O(9) 2.485(5), Ho–O(11) 2.449(6), Ho–O(12) 2.431(6), Ho–O(14) 2.331(5), Zn–O(2) 2.009(4), Zn–O(3) 2.043(5), Zn–O(5) 2.091(6), Zn–N(1) 2.029(6), Zn–N(2) 2.035(6), N(1)–C(8) 1.280(9), N(1)–C(9) 1.48(1), N(2)–C(10) 1.46(1), N(2)–C(11) 1.27(1), O(1)–Ho–O(2) 63.2(2), O(2)–Ho–O(3) 67.6(2), O(3)–Ho–O(4) 64.6(2), O(4)–Ho–O(1) 159.9(2), O(1)–Ho–O(14) 87.3(2), O(4)–Ho–O(14) 81.4(2), O(8)–Ho–O(9) 51.8(2), O(11)–Ho–O(12) 52.0(2), O(2)–Zn–O(3) 77.4(2), O(2)–Zn–N(1) 89.4(2), O(2)–Zn–O(5) 97.5(2), O(2)–Zn–N(2) 152.0(2), O(3)–Zn–O(5) 97.9(2), O(3)–Zn–N(1) 132.9(2), O(5)–Zn–N(1) 128.8(3), N(2)–Zn–O(3) 89.4(2), N(2)–Zn–O(5) 108.7(2), N(2)–Zn–N(1) 81.7(2).

visible emission of compounds **1**–**4**, with lifetimes (τ) ranging from 1.4 to 4.7 ns and quantum yields (Φ_{em}) of $0.72–2.77 \times 10^{-2}$, can be assigned to the intra-ligand emission. The absorption, emission and excitation (monitored at 461 nm) spectra of **1** are shown in Fig. 2. The absorption spectrum of **1** shows that there are three distinct absorption bands, and their absorption intensities are directly proportional to their band energies. This agrees well with the physical fact that the lowest energy states are occupied first, hence, when electrons are excited, it is the highest energy state that can accept the most electrons. The photoluminescence excitation (PLE) spectrum reflects where the maximum contribution of the photoluminescence (PL) comes from. Under steady state conditions, excited electrons relax from the highest excited states to the lowest excited states before they recombine radiatively or non-radiatively. In this case, the PLE spectrum showed exactly this situation; the maximum PL contribution came from the lowest of the excited bands with decreasing contribution from the higher energy band. Thus, although the absorption bands coincide with the excitation bands, as they should, the relative intensities of the energy bands by the two techniques reveals the origin of the physical process measured.

Apart from **2**, compounds **1**, **3** and **4** also exhibit emission corresponding to the lanthanide(III) ion in the NIR region (Fig. 3). These NIR emissions are very similar to those reported for Nd(III), Er(III) and Yb(III).[11] For **1**, the emissions at 875 and 905 nm can be assigned to $^4F_{3/2} \rightarrow {}^4I_{9/2}$, 1068 nm to $^4F_{3/2} \rightarrow {}^4I_{11/2}$ and 1356 nm to $^4F_{3/2} \rightarrow {}^4I_{13/2}$ transitions of Nd(III). For **3** and **4**, the emissions at 1515 and 976 nm can be assigned to the $^4I_{13/2} \rightarrow {}^4I_{15/2}$ transition of Er(III) and $^2F_{5/2} \rightarrow {}^2F_{7/2}$ transition of Yb(III), respectively. The solid state NIR emission spectra of compounds **1**, **3** and **4** are almost identical to their solution spectra. This indicates that the solution structures of compounds **1**, **3** and **4** resemble their solid state structures and the emission in solution probably comes from the Zn-Ln bi-metallic species. Due to the limitation of our equipment, we were unable to measure the excitation (monitored at 1515 nm) spectrum and the NIR luminescence lifetime of **3**. Compounds **1** and **4** show very similar excitation (monitored at the NIR emission peak) and absorption spectra. The excitation spectrum of **1** monitored at 875 nm is identical to that monitored at 461 nm. The NIR luminescence lifetime is 1330 ns for **1** and 1310 ns for **4**. We were unable to measure the quantum efficiency of the NIR

Table 1 Photophysical data of compounds **1**–**4**[a]

	Absorption	Excitation	Emission
	λ_{max}/nm [log(ε/dm^3 mol^{-1} cm^{-1})]	λ_{exc}/nm	λ_{em}/nm (τ/ns, $\Phi_{em} \times 10^2$)[b]
1	350 (3.69), 272 (4.17)	354, 278	461 (1.4, 0.72), 875 (1330)[c]
2	354 (3.38), 275 (4.32), 231 (4.76)	356, 281	465 (1.7, 1.33)
3	357 (3.51), 277 (4.07)	357, 280	473 (4.7, 2.77), 1515[c,d]
4	367 (3.21), 275 (3.94)	370, 277	476 (3.7, 1.37), 976(1310)[c]

[a] Photophysical measurements were made in CH_3OH solution at room temperature. [b] Quantum yield were determined relative to quinine sulfate in 0.1 N H_2SO_4 ($\Phi = 0.55$). [c] Due to the limitations of the instrument, we were unable to determine the quantum yield of the NIR luminescence of compounds, **1**, **3** and **4** directly. [d] Due to the limitations of the instrument, we were unable to measure the lifetime of the NIR luminescence of compound **3**.

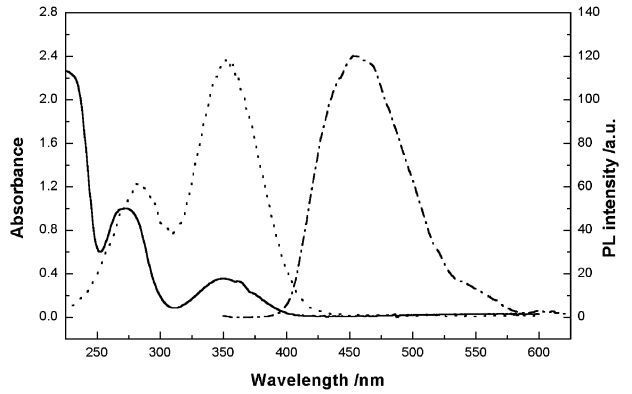

Fig. 2 Room temperature absorption (——), emission (–·–·–) (excited at 337 nm) and excitation (·····) (monotored at either 461 or 875 nm) spectra of **1** in CH_3OH.

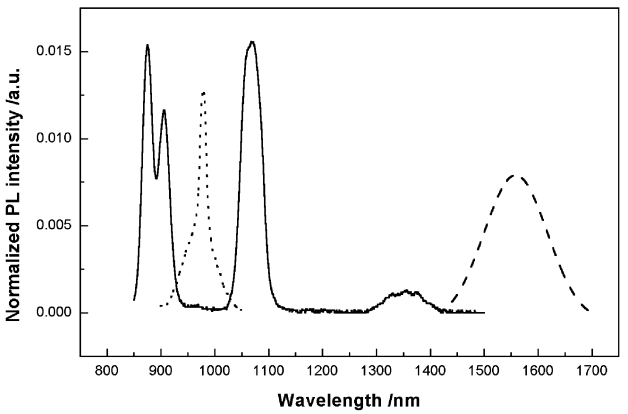

Fig. 3 Room temperature near-infrared luminescence spectrum of **1** (——), **3** (– – –) and **4** (·····) in CH_3OH upon excitation at 355 nm.

luminescence directly; however, we can estimate the maximum possible quantum efficiency of compounds **1**, **3** and **4** by comparing the quantum yield of their antenna (visible emission) with that of the corresponding Zn-Gd complex. This is possible because Gd(III) has no energy levels below 32 000 cm^{-1}, and therefore cannot accept any energy from the antenna. This allows us to study the antenna luminescence in the absence of energy transfer. A similar methodology has been employed to study the NIR luminescence of transition metal-lanthanide bi-metallic complexes.[20] As expected, the quantum yield of the antenna of the Zn-Gd complex (3.37×10^{-2})[24] is higher than that of compounds **1**, **3** and **4**. Assuming 100% energy transfer from the antenna (Zn-Schiff base) to the lanthanide centre, the estimated maximum possible NIR quantum efficiencies for compounds **1**, **3** and **4** are 2.65×10^{-2}, 0.60×10^{-2} and 2.00×10^{-2}, respectively. The actual quantum yields of compounds **1**–**4** will be lower than these values. To ensure that the NIR luminescence is not due to direct excitation of the Ln(III), we also examined the luminescent properties of $Nd(NO_3)_3$ and $[NdL(NO_3)(H_2O)_x]$ in methanol. At the same concentration as **1**, the NIR Nd(III) emission was not observed in the $Nd(NO_3)_3$ case and was only barely observed in the $[NdL(NO_3)(H_2O)_x]$ case.

In this communication we have shown that Zn(II) complexes with a dinucleating Schiff base ligand are good precursors for the preparation of 3d-4f bi-metallic Schiff base complexes, and can act as sensitizers for Nd(III), Er(III) and Yb(III) luminescence in the near-infrared region.

Experimental

Syntheses

Compounds **1**–**4** were prepared by the same procedure. A typical procedure is given for **1**.

$[Zn(NO_3)(\mu\text{-}L)Nd(NO_3)_2(H_2O)]$, 1. When a suspension of $Nd(NO_3)_3 \cdot 6H_2O$ (0.11 g, 0.25 mmol) and ZnL (0.10 g, 0.25 mmol) in methanol (30 cm^3) was heated to 45 °C, it gave a clear solution with the characteristic pale blue colour of Nd(III). The solution was refluxed for 2 h, cooled to room temperature, filtered, concentrated and cooled to −20 °C to give needle-like pale blue crystals. Yield: 0.16 g, 85%, m.p. 230–232 °C. UV-VIS (CH_3OH, 20 °C) λ_{max}/nm [$\log(\varepsilon/dm_3\ mol^{-1}\ cm^{-1})$]: 350 (3.69), 272 (4.17). Fluorescence (CH_3OH, 20 °C) λ_{exc}/nm: 354, 287; λ_{em}/nm: 875, 461. MS (FAB, +ve) m/z: 660 $[M - H_2O - NO_3]^+$, 391 $[ZnL + H]^+$. ESI-MS (CH_3OH) m/z: 660 $[M - H_2O - NO_3]^+$, 472 $[NdL]^+$, 391 $[ZnL + H]^+$. Molar conductivity (CH_3OH, 20 °C) Λ_M: 215 S cm^2 mol^{-1} (c 5.41×10^{-5} M). Anal. calcd (found) for $C_{18}H_{20}N_5O_{14}ZnNd \cdot 0.5CH_3OH$: C, 29.38 (29.73); H, 2.91 (2.65); N, 9.26 (9.17).

$[Zn(NO_3)(\mu\text{-}L)Ho(NO_3)_2(H_2O)]$, 2. $Ho(NO_3)_3 \cdot 5H_2O$ (0.22 g, 0.50 mmol) and ZnL (0.20 g, 0.50 mmol) were used. Yield: 0.35 g, 94%, colourless crystals, m.p. > 230 °C (dec). UV-VIS (CH_3OH, 20 °C) λ_{max}/nm [$\log(\varepsilon/dm^3\ mol^{-1}\ cm^{-1})$]: 354 (3.38), 275 (4.32), 231 (4.76). Fluorescence (CH_3OH, 20 °C) λ_{exc}/nm: 356, 281; λ_{em}/nm: 465. MS (FAB, +ve) m/z: 679 $[M - H_2O - NO_3]^+$, 391 $[ZnL + H]^+$. ESI-MS (CH_3OH) m/z: 679 $[M - H_2O - NO_3]^+$, 492 $[HoL]^+$, 391 $[ZnL + H]^+$. Molar conductivity (CH_3OH, 20 °C) Λ_M: 206 S cm^2 mol^{-1} (c 2.51×10^{-4} M). Anal. calcd (found) for $C_{18}H_{20}N_5O_{14}ZnHo \cdot 1.5H_2O$: C, 27.43 (27.47); H, 2.92 (2.77); N, 8.89 (8.95).

$[Zn(NO_3)(\mu\text{-}L)Er(NO_3)_2(H_2O)]$, 3. $Er(NO_3)_3 \cdot 5H_2O$ (0.11 g, 0.25 mmol) and ZnL (0.10 g, 0.25 mmol) were used. Yield: 0.16 g, 85%, yellow crystals, m.p. > 170 °C (dec). UV-VIS (CH_3OH, 20 °C) λ_{max}/nm [$\log(\varepsilon/dm^3\ mol^{-1}\ cm^{-1})$]: 357 (3.51), 277 (4.07), 231 (4.55). Fluorescence (CH_3OH, 20 °C) λ_{exc}/nm: 357, 280; λ_{em}/nm: 1515, 473. MS (FAB, +ve) m/z: 680 $[M - H_2O - NO_3]^+$, 391 $[ZnL + H]^+$. ESI-MS (CH_3OH) m/z: 680 $[M - H_2O - NO_3]^+$, 494 $[ErL]^+$, 391 $[ZnL + H]^+$. Molar conductivity (CH_3OH, 20 °C) Λ_M: 212 S cm^2 mol^{-1} (c 2.26×10^{-4} M). Anal. calcd (found) for $C_{18}H_{20}N_5O_{14}ZnEr \cdot 2CH_3OH$: C, 29.03 (29.02); H, 3.38 (2.96); N, 8.47 (8.27).

$[Zn(NO_3)(\mu\text{-}L)Yb(NO_3)_2(H_2O)]$, 4. $Yb(NO_3)_3 \cdot 5H_2O$ (0.22 g, 0.50 mmol) and ZnL (0.20 g, 0.50 mmol) were used. Yield: 0.35 g, 94%, yellow solid, m.p. > 230 °C (dec). UV-VIS (CH_3OH, 20 °C) λ_{max}/nm [$\log(\varepsilon/dm^3\ mol^{-1}\ cm^{-1})$]: 367 (3.21), 275 (3.94). Fluorescence (CH_3OH, 20 °C) λ_{exc}/nm: 370, 277; λ_{em}/nm: 976, 476. MS (FAB, +ve) m/z: 706 $[M - NO_3]^+$, 688 $[M - H_2O - NO_3]^+$, 391 $[ZnL + H]^+$. ESI-MS (CH_3OH) m/z: 688 $[M - H_2O - NO_3]^+$, 500 $[YbL]^+$, 391 $[ZnL + H]^+$. Molar conductivity (CH_3OH, 20 °C) Λ_M: 250 S cm^2 mol^{-1} (c 1.35×10^{-4} M). Anal. calcd (found) for $C_{18}H_{20}N_5O_{14}ZnYb \cdot 0.5CH_3OH$: C, 28.30 (28.47); H, 2.80 (2.78); N, 8.92 (8.90).

Photophysical measurements

Steady-state visible fluorescence and PL excitation spectra were recorded on a Photon Technology International (PTI) Alphascan spectrofluorometer and visible decay spectra on a pico-N_2 laser system (PTI Time Master) with $\lambda_{exc} = 337$ nm. NIR emission was detected by a liquid nitrogen cooled InSb IR detector (EG & G) with a preamplifier and recorded by a

lock-in amplifier system. The third harmonics, 355 nm line of a Nd:YAG laser (Quantel Brilliant B) was used as excitation light and was also used to pump the OPO (Opotek MagicPrism VIR) to provide a continuously tunable laser source from 410–670 nm with a pulse width of 4 ns. NIR decay spectra were detected by an Oriel 77343 photomultiplier and captured by a HP54522A 500 MHz oscilloscope. The emission spectra have been corrected for the spectral response of the instrument.

X-Ray crystallography

Colourless crystals of complex **2** suitable for X-ray diffraction experiments were grown by slow evaporation of its solution in *n*-hexane–CH_2Cl_2 at room temperature. Geometric and intensity data were collected at 298 K on a Rigaku AFC7R diffractometer equipped with graphite-monochromated Mo-Kα radiation ($\lambda = 0.71073$ Å). Lorentz-polarization and Ψ-scan absorption corrections were applied to all the intensity data.[25] The structure was solved by a combination of direct methods (SIR 92)[26] and Fourier-difference techniques. All atoms were refined on F by full-matrix least-squares analysis. The hydrogen atoms were placed in their idealized positions (C–H 0.95 Å). All calculations were performed on a Silicon Graphics computer using the program package TEXSAN.[27]

Crystal data for **2**: $C_{18}H_{20}N_5O_{14}ZnHo$, colourless block, $0.25 \times 0.26 \times 0.29$ mm^3, $M = 760.69$, monoclinic, $P2_1/n$ (no. 14), $a = 7.810(2)$, $b = 19.273(2)$, $c = 16.189(3)$ Å, $\beta = 91.99(2)^\circ$, $U = 2435.2(7)$ Å^3, $Z = 4$, $T = 298$ K, μ(Mo-Kα) = 42.97 cm^{-1}, 3603 reflections measured, 3322 unique, R(int) = 0.048, final $R = 0.033$, $Rw = 0.037$ (based on F) for 2563 [$I > 1.5\sigma(I)$] observed reflections.

CCDC reference number 156611. See http://www.rsc.org/suppdata/nj/b1/b104175b/ for crystallographic data in CIF or other electronic format.

Acknowledgements

We thank Dr C. W. Tsang of the Hong Kong Polytechnic University for running and interpreting the ESI-MS spectra. Thanks are due to the Hong Kong Baptist University and the Hong Kong Research Grants Council (HKBU 2023/00P) for financial support.

Notes and references

† Conductivities of **2** in methanol were measured between 4.23×10^{-3} M and 2.71×10^{-5} M. Λ_0 was obtained by extrapolating the slope of the plot of Λ_e *vs.* $\sqrt{C_{eq}}$ to $\sqrt{C_{eq}} = 0$. Then the value of Λ_0 was used to construct the plot $(\Lambda_0 - \Lambda_e)$ *vs.* $\sqrt{C_{eq}}$.

1 P. Caravan, J. J. Ellison, T. J. McMurry and R. B. Lauffer, *Chem. Rev.*, 1999, **99**, 2293.
2 *Bioanalytical Applications of Labelling Technologies*, ed. I. Hemmilä, T. Stählberg and P. Mottram, Wallac Oy, Turku, Finland, 1994.
3 C. Piguet, C. Edder, S. Rigault, G. Bernardinelli, J.-C. G. Bünzil and G. Hopfgartner, *J. Chem. Soc., Dalton Trans.*, 2000, 3999 and references therein.
4 O. Kahn, *Acc. Chem. Res.*, 2000, **33**, 647.
5 C. Piguet and J.-C. G. Bünzli, *Chem. Soc. Rev.*, 1999, **28**, 347.
6 R. Baggio, M. T. Garland, Y. Moreno, O. Peña, M. Perec and E. Spodine, *J. Chem. Soc., Dalton Trans.*, 2000, 2061.
7 C. Edder, C. Piguet, G. Bernardinelli, J. Mareda, C. G. Bochet, J.-C. G. Bünzli and G. Hopfgartner, *Inorg. Chem.*, 2000, **39**, 5059.
8 (*a*) J.-P. Costes, F. Dahan, A. Dupuis and J.-P. Laurent, *Inorg. Chem.*, 1997, **36**, 3429; (*b*) J.-P. Costes, F. Dahan, A. Dupuis and J.-P. Laurent, *Chem. Eur. J.*, 1998, **9**, 1617; (*c*) J.-P. Costes, F. Dahan and A. Dupuis, *Inorg. Chem.*, 2000, **39**, 165; (*d*) J.-P. Costes, F. Dahan, A. Dupuis and J.-P. Laurent, *Inorg. Chem.*, 2000, **39**, 169; (*e*) J.-P. Costes, F. Dahan and A. Dupuis, *Inorg. Chem.*, 2000, **39**, 5994.
9 Z. Xu, P. W. Read, D. E. Hibbs, M. B. Hursthouse, K. M. A. Malik, B. O. Patrick, S. J. Rettig, M. Seid, D. A. Summers, M. Pink, R. C. Thompson and C. Orvig, *Inorg. Chem.*, 2000, **39**, 508.
10 W. T. Carnall, in *Handbook on the Physics and Chemistry of Rare Earths*, ed. K. A. Gschneidner, Jr. and L. Eyring, Elsevier, Amsterdam, 1987, vol. 3, p. 171.
11 S. I. Klink, G. A. Hebbink, L. Grave, F. C. J. M. van Veggel, D. N. Reinhoudt, L. H. Slooff, A. Polman and J. W. Hofstraat, *J. Appl. Phys.*, 1999, **86**, 1181.
12 X.-P. Yang, C.-Y. Su, B.-S. Kang, X.-L. Feng, W.-L. Xiao and H.-Q. Liu, *J. Chem. Soc., Dalton Trans.*, 2000, 3253.
13 M. H. V. Werts, R. H. Woudenberg, P. G. Emmerink, R. van Gassel, J. W. Hofstraat and J. W. Verhoeven, *Angew. Chem., Int. Ed.*, 2000, **39**, 4542.
14 M. Elhabiri, R. Scopelliti, J.-C. G. Bünzli and C. Piguet, *J. Am. Chem. Soc.*, 1999, **121**, 10 747.
15 J. J. Lessmann and W. D. Horrocks, Jr., *Inorg. Chem.*, 2000, **39**, 3114.
16 A. Beeby, R. S. Dickins, S. Faulkner, D. Parker and J. A. G. Williams, *Chem. Commun.*, 1997, 1401.
17 W. D. Horrocks, Jr., J. P. Bolender, W. D. Smith and R. M. Supkowski, *J. Am. Chem.*, 1997, **119**, 5972.
18 M. I. Gaiduk, V. V. Grigoryants, A. F. Mironov, V. D. Rumyantseva, V. I. Chissov and G. M. Sukhin, *J. Photochem. Photobiol. B*, 1990, **7**, 15.
19 (*a*) M. H. V. Werts, J. W. Verhoeven and J. W. Hofstraat, *J. Chem. Soc., Perkin Trans. 2*, 2000, 433; (*b*) M. H. V. Werts, J. W. Hofstraat, F. A. J. Geurts and J. W. Verhoeven, *Chem. Phys. Lett.*, 1997, **276**, 196.
20 S. I. Klink, H. Keizer and F. C. J. M. van Veggel, *Angew. Chem., Int. Ed.*, 2000, **39**, 4319.
21 Y. Hamada, T. Sano, M. Fujita, T. Fujii, Y. Nishio and K. Shibata, *Jpn. J. Appl. Phys.*, 1993, **32**, L511.
22 J. A. Connor, M. Charlton, D. C. Cupertino, A. Lienke, M. McPartlin, I. J. Scowen and P. A. Tasker, *J. Chem. Soc., Dalton Trans.*, 1996, 2835.
23 (*a*) R. D. Feltham and R. G. Hayter, *J. Chem. Soc.*, 1964, 4587; (*b*) R. K. Boggess and D. A. Zatko, *J. Chem. Educ.*, 1975, **52**, 649; (*c*) D. P. Rillema, R. W. Callahan and K. B. Mack, *Inorg. Chem.*, 1982, **21**, 2589.
24 H. S. He, W. K. Wong, K. F. Li and K. W. Cheah, unpublished results.
25 A. C. T. North, D. C. Phillips and F. S. Mathews, *Acta Crystallogr., Sect. A*, 1968, **24**, 351.
26 G. M. Sheldrick, in *Crystallographic Computing 3*, ed. G. M. Sheldrick, C. Kruger and R. Goddard, Oxford University Press, London, 1985, p. 175.
27 TEXSAN, Crystal Structure Analysis Package, Molecular Structure Corporation, Houston, TX, 1985 and 1992.